MJFAS
Malaysian Journal of Fundamental and Applied Sciences

Fathi *et al.* | Malaysian Journal of Fundamental and Applied Sciences, Vol. 21 (2025) 1823-1831

RESEARCH ARTICLE

Graph Theoretical Approach to Topological Features of Zeolitic Tetrahedral Imidazolate Framework-3

Abdelli Fathi[a], Tony Augustine[b], Mohamad Nazri Husin[a]*, J. Sahaya Vijay[c], Jain Maria Thomas[d], S. Roy[c]

[a]Special Interest Group on Modeling and Data Analytics (SIGMDA), Faculty of Computer Science and Computer, Universiti Malaysia Terengganu, Kuala Nerus 21030, Terengganu, Malaysia; [b]Department of Mathematics, Nirmala College (Autonomous), Muvattupuzha, Ernakulam, Kerala, India 686661; [c]Department of Mathematics, Vellore Institute of Technology, Vellore 632014, India; [d]Department of Chemistry, St. George's College, Aruvithura, Kerala 686122, India

Abstract A subclass of metal-organic frameworks (MOFs) known as zeolitic imidazolate frameworks (ZIFs) has drawn a lot of interest because of its capacity to create useful materials via thermal processing. Their capacity to transport electrons and respond to light is improved by this change, which makes them attractive options for photocatalytic uses. When ZIFs are thermally treated, they can be combined to create composites, heterostructures with other semiconductors, or materials with enhanced redox, charge-transfer, and light-capturing capabilities. Due to the dearth of theoretical characterisation predictions in the literature, we concentrate on tetrahedral imidazolate framework-3 (TIF-3), a well-known family of ZIFs, in this work. We fill this gap by using topological indices to reduce the intricacy of TIF-3's two-dimensional structure and methodically list all of its characteristics. Lastly, by establishing a statistical link with the TIF-3 features obtained through experimentation, we validate these attributes.

Keywords: Zeolitic Tetrahedral Imidazolate, edge partition, molecular descriptors, structural-properties, topological indices.

Introduction

Crystalline microporous zeolites are essential to the world economy because they are utilized in various applications in industry such as gas separation, water purification, petrochemical cracking etc. [1]. While zeolites are made from aluminosilicate units linked by oxygen atoms forming diverse frameworks, the challenge of integrating transition metal ions and organic units into their structure for enhanced catalytic applications remains largely unmet [2]. Zeolite imidazolate frameworks ($ZIFs$), a new subclass of metal organic frameworks ($MOFs$), represent a novel category of highly porous materials that blend the benefits of both zeolites and traditional $MOFs$ [7]. They possess zeolite-like topologies, consisting of transition metals as tetrahedral nodes and imidazolate units as linkers [3]. These linkers, through their nitrogen atoms, tetrahedrally coordinate with the metal ions, forming a three-dimensional network [3]. They offer an advantage over zeolites due to their mixed framework, which allows for greater flexibility in surface modification along with high surface areas, large pore volumes, and adjustable pore sizes [4]. $ZIFs$ possess outstanding chemical and thermal stability [6], making them ideal for applications such as gas storage, separation, catalysis, and chemical sensing. Their high porosity and tenable pore chemistry further enhance their potential in these areas [4].

The structure of a ZIF is mainly determined by the type of imidazolate and solvent used, with functionalized imidazolate ligands allowing for greater structural diversity [5]. Ligand-ligand interactions in metal imidazolates are key to controlling framework topology. These interactions can be tailored by modifying the substituents on the imidazolate ring or by combining different imidazolate ligands [8]. Tao *et al*. synthesized five zeolitic structures (Tetrahedral Imidazolate Framework-2 ($TIF-2$) to Tetrahedral

***For correspondence:**
nazri.husin@umt.edu.my

Received: 11 Jan. 2025
Accepted: 25 Feb. 2025

Imidazolate Framework-5 ($TIF-5$)) using a mixed-ligand approach [8]. These structures feature four types of 4-connected topology, achieved by combining a small imidazole ligand with a larger ligand like 5-methylbenzimidazole or 5,6-dimethylbenzimidazole. $TIF-2$ and Tetrahedral Imidazolate Framework-3 ($TIF-3$) feature cubic double four-ring ($d4R$) units, similar to those in industrially important zeolite A. However, in $TIF-2$ and $TIF-3$, these $d4R$ units form unique topologies that differ significantly from their arrangement in zeolite A. TIF-3 is the first metal imidazolate with a distorted body-centred cubic (bcc) arrangement of $d4R$ units, featuring a unique ACO topology previously unseen in metal imidazolates. Zeolitic frameworks with ACO topology is increasingly significant in research due to their unique properties and versatile applications. For example, the zeolitic ACO framework in 3D $MOFs$ based on lithium cubane demonstrates high thermal stability up to $520°C$, while also enabling reversible adsorption of H_2, N_2, and CO_2 [9]. So, in this study we have selected $TIF-3$ zeolite imidazolate framework for the topological studies.

A branch of mathematical chemistry called chemical graph theory offers a strong foundation for describing and interpreting chemical structures using graph-theoretic ideas. This method represents a molecule as a molecular graph, with edges representing chemical bonds and vertices (nodes) representing atoms [10-11]. A greater comprehension of the connections between molecular structure and chemical characteristics is made possible by this abstraction, which makes it possible to investigate molecular behaviours and properties using mathematical techniques from graph theory. Chemical graph theory has become a vital tool for contemporary chemists as the field shifts towards more computational and predictive models [12-15].

The topological index, a numerical number obtained from a molecule's graph representation that reflects its structural features, is one of the fundamental ideas of chemical graph theory. These indices are helpful in predicting molecular behaviours without requiring lengthy laboratory tests, which saves time and money [16-17]. They enable researchers to correlate molecular graphs with physical and chemical qualities including boiling point, stability, and reactivity. Topological indices come in a variety of forms, each concentrating on a particular structural feature of molecular graphs, like atom distances, vertex degrees, or edge connectivity [18-19]. Degree-based topological indices are particularly notable among them due to their ease of use and efficacy in simulating molecular characteristics. This molecular graph's degree of vertices, which represents the quantity of chemical bonds each atom creates, is the basis for computing these indexes. Some well-known examples are the Randic index, which is based on the degree of adjacent vertices and is frequently used in quantitative structure-activity relationships (QSAR) studies, drug design, and materials development due to its straightforward calculation and strong correlation with chemical properties [20-23].

Another important idea in chemical graph theory is graph entropy, which comes from information theory and gives an indication of the degree of disorder or structural complexity in a molecular graph, in addition to topological indices. A molecule's atom and bond configuration are reflected by its graph entropy, which ranges from high to low. A higher entropy indicates a more complicated and unpredictable structure, while a lower entropy indicates one that is more ordered and regular [24-27]. Understanding molecular variety, chemical reaction pathways, and biological networks has been shown to benefit from the application of graph entropy. For example, it can evaluate the diversity of molecular libraries used in drug development or estimate the complexity of metabolic processes. Graph entropy plays a major role in bioinformatics, where it is employed to examine protein-protein interaction networks and metabolic pathways, helping to find essential regulatory nodes critical to system functionality [28-30]. It is particularly effective in analysing huge molecular systems. Calculating the structural complexity of molecules helps distinguish isomers, which are molecules with the same chemical formula but different structural arrangements [31].

In chemistry and related domains, the combined use of topological indices and graph entropy has created new research opportunities. In environmental chemistry, these mathematical methods help evaluate chemical pollutants, help design materials with desired qualities and speed up the screening of molecular libraries in drug discovery [32-34]. A thorough grasp of their mathematical underpinnings and real-world applications is still lacking, despite their potential. By modelling and forecasting molecular attributes using degree-based topological indices and graph entropy, this work seeks to close this gap. Researchers can improve chemical processes, find new materials more quickly, and understand complex molecular systems better by utilising these indices. To improve chemical graph theory's prediction capacity and broaden its applicability to other scientific fields, this research gap must be filled.

Tetrahedral Imidazolate Framework-3

$TIF-3$ is known as Tetrahedral Imidazolate Framework-3, shown in Figure 1. Five zeolitic structures (three different $TIFs$ and two ligands) were prepared by Tao *et al*. [8]. These five different zeolitic structures reveal that they are joined with four types of 4-connected structures and two complementary ligands. The attractive characteristic of $TIF-3$ is its double four-ring units ($4dr$), whose presence is significant at the industrial level. $TIF-3$ features 4-connected tetrahedral frameworks, which include arrangements of distorted body-centred cubic (bcc) $4dr$ units, a configuration not previously found in metal imidazolates.

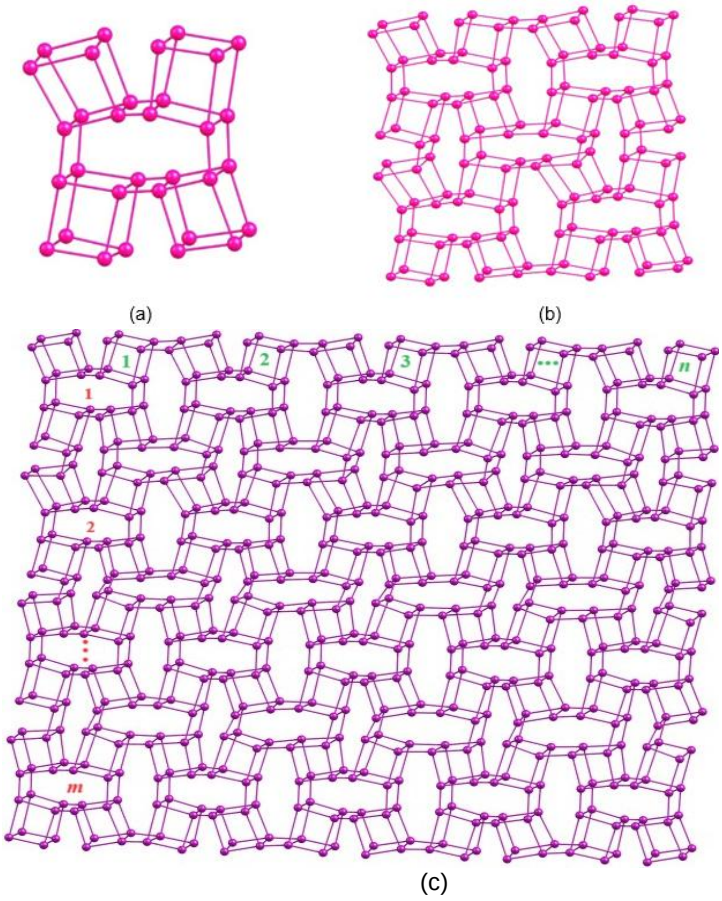

Figure 1. $TIF-3$ Framework a) Unit cell of $TIF-3$, b) $TIF-3(2,2)$, c) A large scale Tetrahedral Imidazolate Framework-3 $TIF-3\ (m,n)$

Additionally, other $TIFs$ have 4-connected tetrahedral frameworks, offering a unique opportunity in the self-assembly process. Unit cell of $TIF-3$ extend to 2D sheet which is observe to feel difficult for involving in synthesize process experimentally so that we synthesized it physically based on graph theoretical approach. The extend to 2D sheet of $TIF-3$ considered as $TIF-3(m,n)$ in this study (See Figure 1(c)). Additionally, it comes to known as $TIF-3\ (2,2)$ (See Figure 1(b)) which is already synthesis in previous literature of Tao *et al* [8]. Therefore, this study about $TIF-3$ where the features of it should aid in its identification in metal imidazolates.

Methodologies

In this paper, we consider a molecular graph $G=(V(G),E(G))$ without loops and multiple edges, where $V\ (G)$ is the set of vertices of G and $E(G)$ is the set of edges of G. Figure 2 provides the workflow of the methodology. The following topological indices given below are investigated in this study. Topological descriptors based on additive degrees are often used to examine the structural differences across molecular systems. In this work, the following noteworthy additive degree-based descriptors from Table 1 are used in this study to achieve our proposed results.

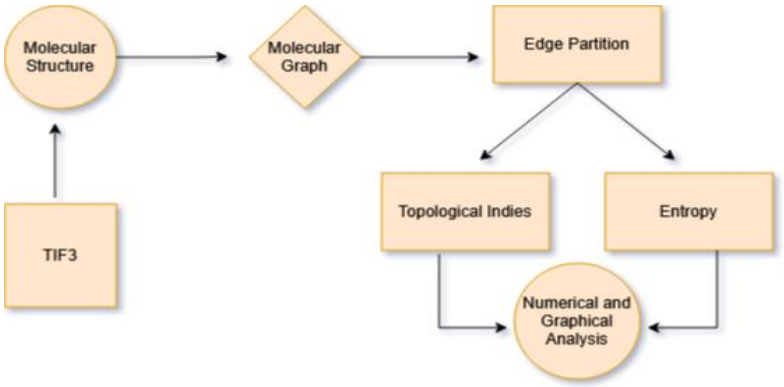

Figure 2. Working methodologies

Table 1. Topological Descriptor (TD) Formula [10-34]

S. No.	TD	Formula
1	First Zagreb index	$M_1(G) = \sum_{v \in V(G)} (d_u + d_v)$
2	Second Zagreb index	$M_2(G) = \sum_{uv \in E(G)} d_u d_v$
3	Reduced second Zagreb index	$RM_2(G) = \sum_{uv \in E(G)} (d_u - 1)(d_v - 1)$
4	Hyper Zagreb index	$HM(G) = \sum_{uv \in E(G)} (d_u + d_v)^2$
5	Augmented Zagreb index	$AZ(G) = \sum_{uv \in E(G)} \left[\frac{d_u d_v}{d_u + d_v - 2}\right]^3$
6	Randic index	$R(G) = \sum_{uv \in E(G)} \left[\frac{1}{\sqrt{d_u d_v}}\right]$
7	Reciprocal Randic index	$RR(G) = \sum_{uv \in E(G)} \sqrt{d_u d_v}$
8	Reduced Reciprocal Randic index	$RRR(G) = \sum_{uv \in E(G)} \sqrt{(d_u - 1)(d_v - 1)}$
9	Harmonic index	$H(G) = \sum_{v \in V(G)} \frac{2}{d_u + d_v}$
10	Sum-Connectivity index	$SC(G) = \sum_{uv \in E(G)} \frac{1}{\sqrt{d_u + d_v}}$
11	Geometric Harmonic index	$GH(G) = \sum_{uv \in E(G)} (d_u^2 + d_v^2 + d_u d_v)$
12	Inverse Sum Index	$IS(G) = \sum_{uv \in E(G)} \frac{d_u d_v}{d_u + d_v}$
13	Forgotten Index	$F(G) = \sum_{uv \in E(G)} {d_u}^2 + {d_v}^2$
14	Symmetric Division Index	$SD(G) = \sum_{uv \in E(G)} \frac{{d_u}^2 + {d_v}^2}{d_u d_v}$
15	Atom Bond Connectivity Index	$ABC(G) = \sum_{uv \in E(G)} \sqrt{\frac{d_u + d_v - 2}{d_u d_v}}$

A graph theory method called edge set partition $(E_{u,v})$ divides a graph's edges into discrete subsets. Topological indices are numbers associated with a graph that provide information about its topological structure. The computation and interpretation of these indices can be greatly impacted by the edge partitioning mechanism. In this manner, the edge set partitions of $TIF-3$ are enumerated below in Table 2.

Table 2. Edge set partitions of $TIF-3$ molecular graph

(m,n)	$E_{u,v}$
$(3,3)$	$4m+4n+8$
$(3,4)$	$16m+8n-8$
$(4,4)$	$64mn-24m-16n$

Result and Discussion

In this section, we used the information which are discussed in the above sections to enumerate the degree-based topological indices expressions. Theorem 1 states the expressions of degree-based indices and Theorem 2 states the expressions of degree-based entropy.

Theorem 1*:* Let G be a large scale Tetrahedral Imidazolate Framework-3 with m,n parameters $TIF-3\ (m,n)$. Then

1. $M_1 = 512mn - 48n - 56m - 8$
2. $M_2 = 1024mn - 124n - 156m - 24$
3. $RM_2 = 576mn - 80n - 104m - 16$
4. $R = 16mn - \frac{8}{3}n - \frac{14}{3}m + \sqrt{3}\left(\frac{16m+8n-8}{6}\right) + \frac{8}{3}$
5. $RR = 256mn - 52n - 84m + 2\sqrt{3}\left(\frac{16m+8n-8}{6}\right) + 24$
6. $RRR = 192mn - 40n - 64m + \sqrt{6}\ (16m + 8n + 8)$
7. $AZ = \frac{32768}{27}mn - \frac{7951657n}{54000} - \frac{3390563m}{18000} - \frac{19467}{1000}$
8. $HM = 4096mn - 488n - 608m - 104$
9. $H = 16mn - \frac{8n}{21} - \frac{2m}{21} + \frac{2}{21}$
10. $GA = 64mn - 12n - 20m + 4\sqrt{3}\left(\frac{16m+8n-8}{7}\right) + 8$
11. $SC = \sqrt{6}\ \left(\frac{4m+4n+8}{6}\right) + \sqrt{7}\left(\frac{16m+8n-8}{7}\right) - \sqrt{2}\left(\frac{24m+16n-64mn}{4}\right)$
12. $AZI = 128mn - \frac{22n}{3} - \frac{20m}{3} - \frac{2}{3}$
13. $IS = 128mn - \frac{86n}{7} - \frac{102m}{7} - \frac{12}{7}$
14. $ABC = \sqrt{3}\left(\sqrt{8mn - 2n - 3m}\right) + \frac{20m}{3} + \frac{10n}{3} - \sqrt{\frac{10}{3}} + \sqrt{\frac{16m}{9} + \frac{16n}{9} + \frac{32}{9}}$
15. $F = 2048mn - 240n - 296m - 56$

Theorem 2*:* Let G be a large scale Tetrahedral Imidazolate Framework-3 with with m,n parameters $TIF-3\ (m,n)$. Then

1. $EM_1 = log\ (512mn - 48n - 56m - 8) - ((9732603338693273m/70368744177664 + 64286251046835705n/562949953421312 - 4682486076124019mn/4398046511104 + 12928997887555669/562949953421312)/\ (56m + 48n - 512mn + 8))$
2. $EM_2 = log\ (1024mn - 124n - 156m - 24) - ((286244236810184397m/562949953421312 + 220750460173321381n/562949953421312 - 6243314768165359mn/2199023255552 + 22616758927381113/281474976710656)/\ (156m + 124n - 1024mn + 24))$
3. $ERM_2 = log\ (576mn - 96n - 136m) - ((39464324349307927m/140737488355328 + 58607361487641809n/281474976710656 - 44529389044833123mn/35184372088832 + 1465184037191045/35184372088832)/\ (136m + 96n - 576mn))$
4. $EHM = log\ (4096mn - 488n - 608m - 104) - ((396996610227317639m/140737488355328 + 624051413597677621n/281474976710656 - 4682486076124019mn/274877906944 + 138919188880607839/281474976710656)/\ (608m + 488n - 4096mn + 104))$
5. $EAZ = log\ (32768mn/27 - 7951657n/54000 - 3390563m/18000 - 19467/1000) - ((29156115642899708406 91m/4503599627370496000 + 6640139390859322133849n/$

$1351079888211148800 - 368105188198141mn/103079215104 + 154859578708088493171/225179981368524800)/ (3390563m/18000 + 7951657n/54000 - 32768mn/27 + 19467/1000))$

6. $ER = log\,(16mn - 8n/3 - 14m/3 + sqrt\,(3)\,(16m + 8n - 8)/6 + 8/3) + ((6243314768165359mn/281474976710656 - 6891117205312865n/1688849860263936 - 46294413125747537m/6755399441055744 + 1398878082754463\,sqrt\,(3)\,(16m + 8n - 8)/6755399441055744 + 4947709893870347/1688849860263936)/ (16mn - 8n/3 - 14m/3 + sqrt\,(3)\,(16m + 8n - 8)/6 + 8/3))$
7. $ERR = log\,(256mn - 28n - 36m) + ((6243314768165359mn/17592186044416 - 42524953304517353n/562949953421312 - 67498212377178789m/562949953421312 + 5595512331017853\,sqrt\,(3)\,(16m + 8n - 8)/2251799813685248 + 7421564840805519/281474976710656)/ (36m + 28n - 256mn))$
8. $ERRR = log\,(192mn - 40n - 64m + sqrt\,(6)\,(16m + 8n - 8) + 16) - ((7421564840805519mn/35184372088832 - 53129203958278793n/1125899906842624 - 82815463321500869m/1125899906842624 + 4034683638976513\,sqrt\,(6)\,(16m + 8n - 8)/4503599627370496 + 6243314768165359/562949953421312)/ (192mn - 40n - 64m + sqrt\,(6)\,(16m + 8n - 8) + 16))$
9. $EH = log\,(16mn - 8n/21 - 2m/21 + 8/21) + ((53247635651466551m/47287796087390208 + 14386163408594279n/11821949021847552 - 6243314768165359mn/281474976710656 - 782312228496653/11821949021847552)/ (2m/21 + 8n/21 - 16mn - 8/21))$
10. $ESC = log(sqrt(6)(4m + 4n + 8)/6 + sqrt(7)(16m + 8n - 8)/7 - sqrt(2)(24m + 16n - 64mn)/4) + ((8069367277953025sqrt(6)(4m + 4n + 8)/54043195528445952 + 1095450027772747sqrt(7)(16m + 8n - 8)/7881299347898368 - 1170621519031005sqrt(2)(24m + 16n - 64mn)/4503599627370496)/(sqrt(6)(4m + 4n + 8)/6 + sqrt(7)(16m + 8n - 8)/7 - sqrt(2)(24m + 16n - 64mn)/4))$
11. $EGA = log\,(64mn - 12n - 20m + 4sqrt\,(3)\,(16m + 8n - 8)/7 + 8) + (5943104906424687sqrt\,(3)\,(16m + 8n - 8)/ (1008806316530991104 * (64mn - 12n - 20m + 4sqrt\,(3)\,(16m + 8n - 8)/7 + 8)))$
12. $EIS = log\,(128mn - 86n/7 - 102m/7 - 12/7) - ((25305859159439106 9m/15762598695796736 + 194762151198740057n/15762598695796736 - 6243314768165359mn/70368744177664 + 19911083850948513/7881299347898368)/ (102m/7 + 86n/7 - 128mn + 12/7))$
13. $EAZI = log\,(128mn - 22n/3 - 20m/3 - 2/3) - ((22024277875329695m/6755399441055744 + 59484166484321849n/13510798882111488 - 6243314768165359mn/70368744177664 + 15435610733662459/13510798882111488)/ (20m/3 + 22n/3 - 128mn + 2/3))$
14. $EF = log\,(2048mn - 240n - 296m - 56) - ((82051931442732445m/70368744177664 + 259681734612169487n/281474976710656 - 7804143460206699mn/1099511627776 + 64052905021443727/281474976710656)/ (296m + 240n - 2048mn + 56))$
15. $EABC = log(sqrt(3)sqrt(8mn - 2n - 3m) + sqrt(20m/3 + 10n/3 - 10/3) + sqrt(16m/9 + 16n/9 + 32/9)) + ((7304210039150669m/6755399441055744 + 7304210039150669n/6755399441055744 + 2628507119547695sqrt(3)sqrt(5)(16m + 8n - 8)/36028797018963968 - 4417262258377693 * sqrt(2)sqrt(3)(24m + 16n - 64mn)/36028797018963968)/(sqrt(3) * sqrt(8mn - 2n - 3m) + sqrt(20m/3 + 10n/3 - 10/3) + sqrt(16m/9 + 16n/9 + 32/9))) + (7304210039150669/3377699720527872)/(sqrt(3) * sqrt(8mn - 2n - 3m) + sqrt(20m/3 + 10n/3 - 10/3) + sqrt(16m/9 + 16n/9 + 32/9))$

Numerical Analysis

This section presents the numerical results for degree-based topological descriptors and their entropy-enhanced counterparts for $TIF - 3(m,n)$ structures, with variable values of m and n ranging from 1 to 10. The data were visualized using Origin 2020b software, which allows for a clear comparison of computed descriptors. Tables 3–4 provide a summary of these values, and Figure 3 displays these relationships as 3D plots, highlighting distinctions among the topological indices and entropy for $TIF - 3(m,n)$. Specifically, the 3D graph of topological indices shows the Harmonic index reaching the highest values, while in the entropy graph, the Atom-Bond Connectivity (ABC) index exhibits the highest entropy values, potentially indicating different structural complexities within the $TIF - 3(m,n)$ molecular graph. These findings offer insights into the physical and chemical characteristics of $TIF - 3(m,n)$ structures, making it easier for future researchers to analyze their properties systematically.

Table 3. Numerical values of degree-based topological descriptors

TD	$(1,1)$	$(2,2)$	$(3,3)$	$(4,4)$	$(5,5)$	$(6,6)$	$(7,7)$	$(8,8)$	$(9,9)$	$(10,10)$
M_1	400	1832	4288	7768	12272	17800	24352	31928	40528	50152
M_2	720	3512	8352	15240	24176	35160	48192	63272	80400	99576
RM_2	376	1920	4616	8464	13464	19616	26920	35376	44984	55744
R	15.9521	63.5470	143.1419	254.7367	398.3316	573.9265	781.5214	1021.1	1292.7	1596.3
RR	199.4256	914.5641	2141.7	3880.8	6132	8895	12170	15957	20257	25068
RRR	143.1918	673.9796	1588.8	2887.6	4570.3	6637.1	9087.9	11923	15141	18744
AZ	858.5451	4163.8	9896.3	18056	28643	41657	57099	74968	95264	117990
HM	2896	14088	33472	61048	96816	140776	192928	253272	321808	398536
H	15.9048	15.9048	142.9524	254.4762	398	573.5238	781.0476	1020.5714	1292.0952	1595.6190
GA	55.8359	239.5897	551.3436	991.0974	1558.9	2254.6	3078.4	4030.1	5109.9	6317.6
SC	21.0647	87.1419	198.474	355.0609	556.9027	803.9993	1096.4	1434	1816.8	2244.9
AZI	113.3333	483.3333	1109.3333	1991.3333	3129.3333	4523.3333	6173.3333	8079.3333	10241.3333	12657.3333
IS	99.4286	456.5714	1069.7143	1938.8571	3064	4445.1429	6082.2857	7975.4286	10124.5714	12529.7143
ABC	34.411	140.2069	317.5569	566.4611	886.9195	1.28E + 03	1.74E + 03	2.28E + 03	2.88E + 03	3.56 + 03
F	1456	7064	16768	30568	48464	70456	96544	126728	161008	199384

Table 4. Numerical values of Entropy (Ent)

Ent	$(1,1)$	$(2,2)$	$(3,3)$	$(4,4)$	$(5,5)$	$(6,6)$	$(7,7)$	$(8,8)$	$(9,9)$	$(10,10)$
EM_1	4.0185	5.4767	6.311	6.8978	7.3509	7.7201	8.0316	8.3011	8.5385	8.7507
EM_2	3.9985	5.4661	6.304	6.8926	73468	7.7167	8.0287	8.2985	8.5363	8.7487
ERM_2	3.703	5.32	6.2071	6.8202	7.2889	7.6685	7.9874	8.2625	8.5042	8.7199
EHM	3.9989	5.4666	6.3044	6.893	7.3471	7.7169	8.0289	8.2987	8.5364	8.7489
EAZ	4.0024	5.4671	6.3045	6.8929	7.347	7.7168	8.0288	8.2986	8.5363	8.7488
ER	4.0181	5.4757	6.3101	6.8971	7.3503	7.7196	8.0312	8.3007	8.5382	8.7504
ERR	3.931	5,4283	6.2778	6.8726	7.3306	7.7031	8.017	8.2883	8.5271	8.7404
$ERRR$	4.0117	5.4729	6.3084	6.8959	7.3494	7.7188	8.0305	8.3001	8.5377	8.75
EH	4.0181	5.4759	6.3103	6.8972	7.3504	7.7197	8.0313	8.3008	8.5382	8.7505
ESC	4.0235	5.4795	6.3128	6.8991	7.352	7.721	8.0324	8.3017	8.5391	8.7512
EGA	4.0253	5.4806	6.3135	6.8997	7.3524	7.7213	8.0327	8.302	8.5393	8.7515
EIS	4.0183	5.4764	6.3107	6.8976	7.3507	7.7199	8.0315	8.301	8.5384	8.7506
$EAZI$	4.0252	5.4805	6.3135	6.8997	7.3524	7.7213	8.0326	8.302	8.5393	8.7514
EF	3.9993	5.4672	6.3048	6.8933	7.3474	7.7172	8.0291	8.2989	8.5366	8.749
$EABC$	4.0562	7.3049	10.5275	13.7817	17.0709	20.3919	23.741	27.1148	30.5103	33.9253

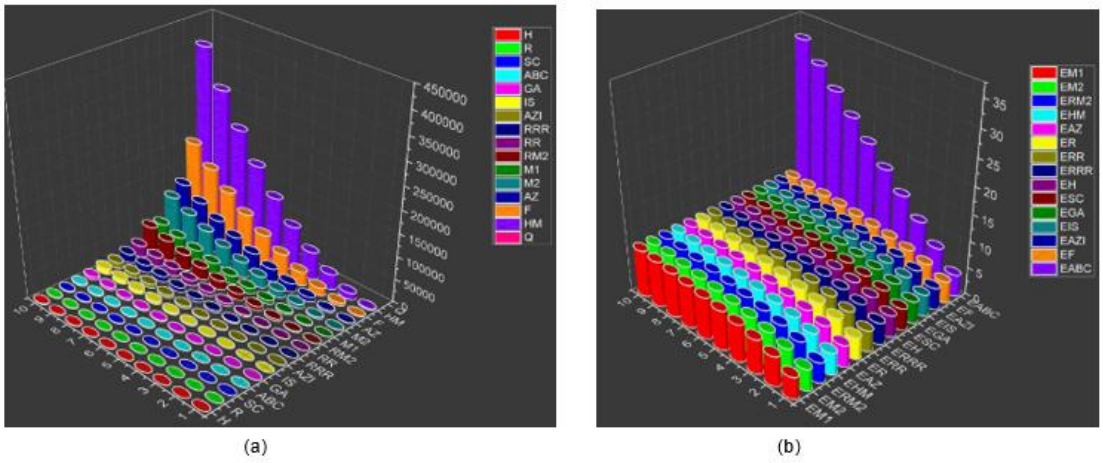

(a) (b)

Figure 3. Graphical representation, a) Relation between degree-based topological indices and parameters of $TIF - 3(m,n)$ b) Relation between degree-based entropy and parameters of $TIF - 3(m,n)$

Conclusions

In this study, degree-based topological indices and entropy measures were computed for $TIF-3(m,n)$ structures. The findings offer a valuable foundation for advancing research and development in $TIF-3(m,n)$ structural studies. By incorporating both degree-based and entropy-enhanced topological descriptors, this work provides a robust framework to facilitate the design of $TIF-3(m,n)$ structures for targeted applications, particularly in materials science and molecular engineering. The graphical representations and numerical comparisons presented here will be valuable to both theoretical chemists and industry professionals, offering insights that clarify the effectiveness of various indices. These observations enable future researchers to select indices with greater precision, optimizing their approaches to exploring and applying $TIF-3(m,n)$ structures. The methods and results outlined in this study pave the way for further exploration across scientific and industrial fields, supporting the development of innovative applications.

Conflicts of Interest

The author(s) declare(s) that there is no conflict of interest regarding the publication of this paper.

Acknowledgement

The authors would like to thanks to Universiti Malaysia Terengganu for the support of this research work.

References

[1] Verma, C., Quraishi, M. A., & Hussain, C. M. (2023). Greenly synthesized zeolites as sustainable materials for corrosion protection: Design, technology and application. *Advances in Colloid and Interface Science, 314*, 102868.
[2] Park, K. S., Ni, Z., Côté, A. P., Choi, J. Y., Huang, R., Uribe-Romo, F. J., Chae, H. K., O'Keeffe, M., & Yaghi, O. M. (2006). Exceptional chemical and thermal stability of zeolitic imidazolate frameworks. *Proceedings of the National Academy of Sciences, 103*(27), 10186–10191.
[3] Kumar, A., Rana, S., Sharma, G., Dhiman, P., Shekh, M. I., & Stadler, F. J. (2023). Recent advances in zeolitic imidazole frameworks based photocatalysts for organic pollutant degradation and clean energy production. *Journal of Environmental Chemical Engineering, 11*(5), 110770.
[4] Kouser, S., Hezam, A., Khadri, M. N., & Khanum, S. A. (2022). A review on zeolite imidazole frameworks: Synthesis, properties, and applications. *Journal of Porous Materials, 29*(3), 663–681.
[5] Fu, F., Zheng, B., Xie, L. H., Du, H., Du, S., & Dong, Z. (2018). Size-controllable synthesis of zeolitic imidazolate framework/carbon nanotube composites. *Crystals, 8*(10), 367.
[6] Bouëssel du Bourg, L., Ortiz, A. U., Boutin, A., & Coudert, F. X. (2014). Thermal and mechanical stability of zeolitic imidazolate frameworks polymorphs. *APL Materials, 2*(12).
[7] Phan, A., Doonan, C. J., Uribe-Romo, F. J., Knobler, C. B., O'Keeffe, M., & Yaghi, O. M. (2010). Synthesis, structure, and carbon dioxide capture properties of zeolitic imidazolate frameworks.
[8] Tao, W., Xianhui, B., Jian, Z., & Pingyun, F. (2008). New zeolitic imidazolate frameworks: From unprecedented assembly of cubic clusters to ordered cooperative organization of complementary ligand. *Chemistry of Materials, 20*, 7377–7382.
[9] Zhao, X., Wu, T., Zheng, S. T., Wang, L., Bu, X., & Feng, P. (2011). A zeolitic porous lithium–organic framework constructed from cubane clusters. *Chemical Communications, 47*(19), 5536–5538.
[10] Jahanbani, A. (2020). On topological indices of carbon nanocones and nanotori. *International Journal of Quantum Chemistry, 120*(6).
[11] Wiener, H. (1947). Structural determination of paraffin boiling points. *Journal of the American Chemical Society, 69*(1), 17–20.
[12] Mhagama, L. S., Nadeem, M. F., & Husin, M. N. (2024). On the edge metric dimension of some classes of cacti. *AIMS Mathematics, 9*(6), 16422–16435.
[13] Rafiullah, M., Dur-E-Jabeen, & Husin, M. N. (2024). Some mathematical properties of sombor indices for regular graphs. *Malaysian Journal of Fundamental and Applied Sciences, 20*(6), 1392–1397.
[14] Fathi, A., Sahaua, V. J., Husin, M. N., & Augustine, T. (2024). Valency-based molecular descriptor on structural property relationship of Ni tetrathiafulvalene tetrathionate. *Malaysian Journal of Fundamental and Applied Sciences, 20*(6), 1398–1409.
[15] Gowtham, K. J., Husin, M. N., & Siddiqui, M. K. (2024). Some new bounds on the modified symmetric division deg index. *Malaysian Journal of Mathematical Sciences, 18*(1), 39–50.
[16] Trinajstic, N. (1992). *Chemical graph theory*. CRC Press.
[17] Todeschini, R., & Consonni, V. (2000). *Handbook of molecular descriptors*. Wiley-VCH.
[18] Nadeem, M., Ahmad, S., Siddiqui, M. K., & Naeem, M. (2019). Topological descriptor of 2-dimensional silicon carbons and their applications. *Open Chemistry, 17*(1), 1473–1482.
[19] Rada, J. (2020). Vertex-degree based topological indices of graphene. *Polycyclic Aromatic Compounds, 42*(4),

1524–1532.
[20] Saleem, H., Husin, M. H., Ali, S., Hameed, M. S., & Ahmad, Z. (2024). Topology of edge contracted Möbius ladder: Indices and dimension. *Malaysian Journal of Fundamental and Applied Sciences, 20*(4), 739–758.
[21] Gowtham, K. J., & Husin, M. N. (2023). A study of families of bistar and corona product of graph: Reverse topological indices. *Malaysian Journal of Mathematical Sciences, 17*(4), 575–586.
[22] Husin, M. N., & Saudi, N. H. A. M. (2024). Investigation of Zagreb indices and Zagreb coindices of line graphs implementing subdivision process. *AIP Conference Proceedings, 2905*(1), 030002. https://doi.org/10.1063/5.0172141
[23] Husin, M. N., Khan, A. R., Awan, N. U. H., Campena, F. J. H., Tchier, F., & Hussain, S. (2024). Multicriteria decision making attributes and estimation of physicochemical properties of kidney cancer drugs via topological descriptor. *PLOS ONE, 19*(5), e0302276. https://doi.org/10.1371/journal.pone.0302276
[24] Rada, J., & Cruz, R. (2014). Vertex-degree-based topological indices over graphs. *MATCH Communications in Mathematical and in Computer Chemistry, 72*, 603–616.
[25] Vijay, J. S., Roy, S., Beromeo, B. C., Husin, M. N., Augustine, T., Gobithaasan, R. U., & Easuraja, M. (2023). Topological properties and entropy calculations of aluminophosphates. *Mathematics, 11*, 2443.
[26] Zuo, X., Shooshtari, H., & Cancan, M. (2023). Entropy measures of topological indices based molecular structure of benzenoid systems. *Polycyclic Aromatic Compounds, 44*(5), 2980–2990.
[27] Husin, M. N., Hasni, R., & Arif, N. E. (2015). Zagreb polynomials of some nanostar dendrimers. *Journal of Computational and Theoretical Nanoscience, 12*(11), 4297–4300.
[28] Gao, W., Husin, M. N., Farahani, M. R., & Imran, M. (2016). On the edges version of atom-bond connectivity and geometric arithmetic indices of nanocones CNCκ[n]. *Journal of Computational and Theoretical Nanoscience, 13*(10), 6741–6746.
[29] Dehmer, M., & Mowshowitz, A. (2011). A history of graph entropy measures. *Information Sciences, 181*(1), 57–78.
[30] Sol, R. V., & Valverde, S. I. (2004). Information theory of complex networks: On evolution and architectural constraints. *Lecture Notes in Physics, 650*, 189–207.
[31] Yu, G., Siddiqui, M. K., & Hussain, M. (2024). On topological indices and entropy measures of beryllonitrene network via logarithmic regression model. *Scientific Reports, 14*, 7187.
[32] Lal, S., Bhat, V. K., & Sharma, S. (2024). Topological indices and graph entropies for carbon nanotube Y-junctions. *Journal of Mathematical Chemistry, 62*, 73–108.
[33] Rahul, M. P., Clement, J., Junias, J. S., Arockiaraj, M., & Balasubramanian, K. (2022). Degree-based entropies of graphene, graphyne and graphdiyne using Shannon's approach. *Journal of Molecular Structure*.
[34] Ghani, M. U., Campena, F. J. H., Pattabiraman, K., Ismail, R., Karamti, H., & Husin, M. N. (2023). Valency-based indices for some succinct drugs by using M-polynomial. *Symmetry, 15*, 603.